Supplementary Material

This pdf file includes:

Supplementary text (Materials and Methods, extended version)

Figures S1-S8

Tables S1-S3

SI References

1 Supplementary Data: Materials and Methods, extended version

1.1 Foraminifera determination

The foraminiferal investigations were carried out based on 100 g of sediments taken from samples collected in the field (without pre-treatment), homogenized and placed in an experiment tray. The foraminifera were removed one by one from the sediments using the tip of a lightly dampened "rigger" type paint brush and a binocular microscope (Nachet Opale 0152). This operation was repeated three times for each sample. The species identification has shown that for all the samples, one single species (*Baculogypsina sphaerulata*) dominates largely (>90%) the foraminiferal assemblage. Radiocarbon dating have been performed exclusively on samples of this species. In each layer, these foraminifera, with tests characterized by prominent radial spines, exhibit different aspects due to wear and tear or alteration. Their shape can vary from stars with sharp spines to spheroids decayed by weathering. During a tsunami, water turbulence reworks ancient sedimentary stocks and mixes elements of different ages. In order to limit dating errors, we have selected only the freshest forms of *Baculogypsina sphaerulata* present in each of the layers to constitute our dating samples.

1.2 Geochemical analysis

Analytical procedures major and trace elements in rock samples

Each sample aliquot: 100mg was mixed with 300mg of LiBO2 flux in porcelain dish, transferred to a graphite crucible machined from 25 mm diameter rods and fused for 5 min at about 1100°C in an induction furnace (2 kW). The melt was poured into a disposable polystyrene beaker containing 50 ml of 1M HNO3 stirred by a magnetic bar. After complete dissolution of the shattered quenched melt droplets (about 15 min), the solution was passed through a filter paper (Whatman, N° 40, 110mm diameter) to remove graphite particles. The final volume was made up to 200 ml with 1 M HNO3. Reference materials GH (for Si, Na, K) and BR (for the other elements), both from CRPG, Nancy, France (Centre Pétrographique et Géochimique), prepared in the same way as the unknown samples, provided high points of the calibration lines, while a pure LiBO2 solution (300 mg in 200 ml M HNO3) was used as the zero in every case.

A ULTIMA-C spectrometer (Horiba scientific, Jobin-Yvon) was used. This instrument combines two spectrometers to measure emission lines from elements excited in a single plasma torch: One polychromator and one scanning monochromator. The polychromator was used for the simultaneous measurement of emission lines from the major elements. The scanning high-resolution monochromator was used for sequential determination of emission lines from alkali elements Na, K and P.

ICP-AES operating conditions:

-incident power: 1.1kW

-reflected power: <15W

-plasma gas flow rate: 16 l/min

-permanent sheath gas flow rate: 0.2 l/min

-additional sheath gas (alkalis): 0.7 l/min

-carrier gas flow rate: 0.8 l/min

-solution uptake: 0.9 l/min Mhammed Benbakkar Laboratoire: Magmas et Volcans

Analysis of melt inclusions, matrix glasses and fluid inclusions

Matrix glasses and fluid inclusions

Pumice samples A17-P-1 and KOL1 were crushed, sieved at 500, 250, and 125 µm, and washed in purified water and hydrochlroric acid (1%) in an ultrasonic bath. Glass grains from the 125-250 µm grainsize fraction were handpicked and mounted in epoxy resin stubs and polished in the Cambridge Tephra Lab at the Department of Geography of the University of Cambridge. Mounted samples were analysed for single glass-shard element oxide compositions with a SX100 CAMECA electron microprobe (EMPA) at the Department of Earth Sciences, University of Cambridge, UK. Major elements were measured with an accelerating voltage of 15 keV, 6 nA and a 10-µm diameter defocused beam. Elements were counted on-peak for 10 s (Na), 20 s (Si), 30s (Ti, Al, Fe, Mg, Ca and K), 40s (Mn), 60 s (Cl), and 90 s (P). Sodium was measured first in order to minimise alkali loss. The analytical accuracy was checked against international standards ATHO-G, STH-S6, KL2-G and an internal standard of peralkaline obsidian from Lipari, (74 wt% SiO2, 3.8 wt% Na2O, 5.3 wt% K2O). Standards compositions and standard deviations are reported in Table SXX. Where possible, we analysed 30-50 points per sample. Detailed normalised compositions free of volatiles are reported in Table XX.

1.3 Radiocarbon dating

Sample preparation

Marine shells were acid-etched with dilute HCl and tested for recrystallization at the Laboratory of Physical Geography (LGP), CNRS, Meudon, France, where standard chemical pre-treatment (ABA), CO2 production and graphitisation of charcoal were also performed.

Measurements

Dating were performed at the DirectAMS Radiocarbon Dating Laboratory in Seattle, USA. Samples then proceed through portioning/subsampling, physical and chemical pre-treatment protocols, production of CO2 by combustion or acid digestion, reduction of CO2 to graphite, preparation of graphite for measurement, measurement of carbon isotopes by Accelerator Mass Spectrometer (AMS), and data analysis. DirectAMS operates National Electrostatics Corporation (NEC) 1.5 SDH Compact Pelletron AMS.

Data calibration

DirectAMS results are not calibrated, nor corrected for the marine reservoir effect, as a number of site-specific calibration curves may be considered. Calibrations were performed by OxCal that incorporate the compilations of INTCAL20. All determinations were calibrated using the terrestrial and marine curves (SHCal20 and Marine20) of Calib Rev. 8.1 (Stuiver et al., 2020). Marine samples originated from the open ocean environments and were therefore calibrated with a DeltaR value of 11+-83 as recommended by Petchey and Clark (2011), or Clark and Reepmeyer (2014).

1.4 Numerical modeling of tsunami caused by caldera-forming eruption and slope failure

For this type of scenario, the modelling was carried out in several phases: (i) creation of a Digital Elevation Model and inventory of the submarine calderas along the Tonga Ridge south of Tongatapu; (ii) 2D reconstruction of the initial shape of these volcanoes before their collapse; (iii) selection of the best candidates for tsunami modelling; (iv) launching of the simulations.

DEM preparation

We selected several sources of DEM data for the baseline data. We identified several available data sources such as GEBCO, GMRT, and NIWA to compare them for the selection of DEM data. The GMRT data was selected as the base data because it brings together several data from various bathymetric data. The digital elevation model using the GMRT map of the South Tonga region (Tofua) is shown in Figure S4. In fact, GMRT has several resolutions combined into one database as mentioned in https://www.gmrt.org/about/ as follows:

a. Ship-based multibeam swath bathymetry data (100-m resolution) from research cruises assessed, cleaned, processed and curated by the MGDS.
b. Gridded seafloor depth data (variety of scales) contributed by the international science community

c. Gridded seafloor depth data (30 arc-second resolution) from the General Bathymetric Chart of the Oceans (GEBCO_2014)
d. Gridded seafloor depth data (2-km resolution) from the International Bathymetric Chart of the Arctic Ocean (IBCAO) version 2.23
e. Gridded seafloor depth data and ice surface data (500 m resolution) from the International Bathymetric Chart of the Southern Ocean (IBCSO)

The quality of the data we use from GMRT was then checked to validate the resolution of the DEM. The GMRT in the South Tonga arc has a resolution of 0.003767 decimal degree units (Figure S4). One decimal degree unit value in the Tonga arc (included in 23N/S) is equal to 102.47 m.

2D cross-section

GMRT provides adequate data for 2D reconstruction. The GMRT global DEM was initially masked to the Tofua area and adjusted to 19 existing volcanoes. Interpolation of the cross-sections was performed using Global Mapper v12 (registered) to extract x, y, z values. At this stage, each cross-section was interpolated through the caldera and volcano slopes along two preferred directions, N-S and W-E. The x,y,z data from the cross-section line was then extracted as .csv data. From this .csv database, which contains x, y, z information, we reconstructed the current and pre-caldera shape of the selected volcanoes.

Volcano Candidate Selection

The initial reconstruction of the volcanic body can be carried out by the interpolation method deduced from the stratigraphic data (Lahitte et al., 2012). As we do not have adequate information about the stratigraphic data, the reconstruction was carried out using the surface fit and trend line from the x, y, z interpolation (Karátson et al. 2016). The result of the 2D reconstruction using the cross-section method shows that the volcanic edifice can be classified into two different types, island volcanoes and submarine volcanoes: (i) Seven undersea calderas resulted from the collapse of an ancient volcanic island. The highest elevation of the ancient volcanic island is the one of Volcano #5a (>1000m), and the lowest is the one of Volcano #5b (<250m. With the highest elevation and widest caldera, Volcano 5a is a good candidate for large tsunami generation, along with Volcano #1 and Volcano #2. (ii) Eight undersea calderas were formed by the collapse of an ancient submarine volcano. The size of these calderas is smaller than the ones of the former volcanic islands, except volcano #18. This category of volcanoes is less likely to have generated a large-scale tsunami.

Tsunami modelling

We carried out two simulations of volcanic tsunamis triggered by voluminous PDCs or debris avalanche using VOLCFLOW code. The first simulation concerns a slope failure of the south flank of Tofua volcano (Figure SX). The second one concerns a 15 km^3 debris avalanche entering the sea from the Volcano #2 before the total collapse of the former cone (Figure SX).

2 Supplementary Figures and Tables

For more information on Supplementary Material and for details on the different file types accepted, please see here. Figures, tables, and images will be published under a Creative Commons CC-BY licence and permission must be obtained for use of copyrighted material from other sources (including re-published/adapted/modified/partial figures and images from the internet). It is the responsibility of the authors to acquire the licenses, to follow any citation instructions requested by third-party rights holders, and cover any supplementary charges.

2.1 Supplementary Figures

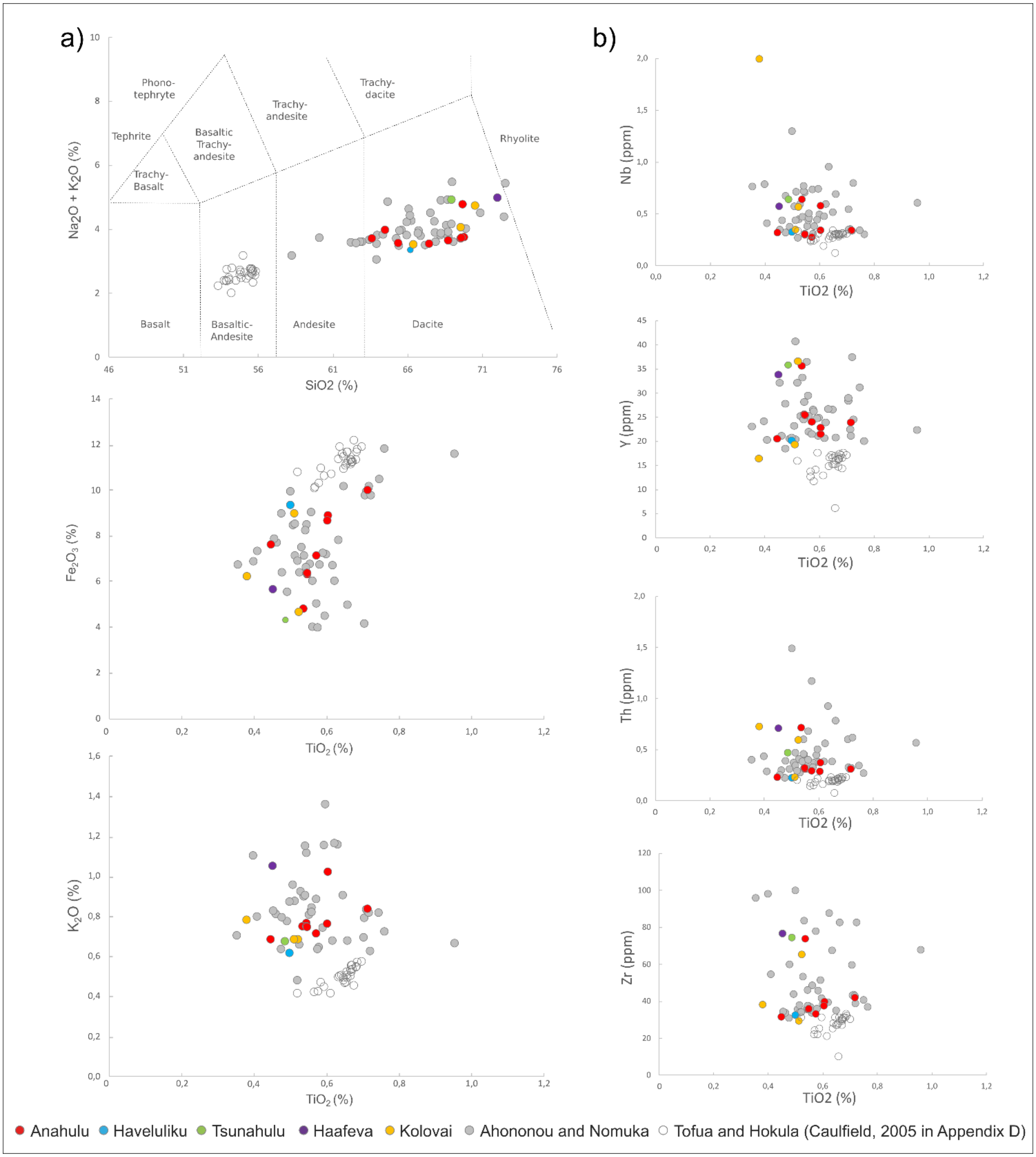

Fig. S1. Geochemistry of pumice rocks (bulk rock) within inferred tsunami deposits in Tongatapu. (a) Major elements. (b) Trace elements. The dacitic composition is representative of the volcanoes along the Tonga-Kermadec Trench. It differs, on the one hand from most other circum-Pacific andesite-dacite suites in their very low content of alkali, especially low K_2O, on the other hand from the basalt-andesite ignimbrites formed during the latest paroxysmal eruption of Tofua volcano ca. 1000 yrs BP.

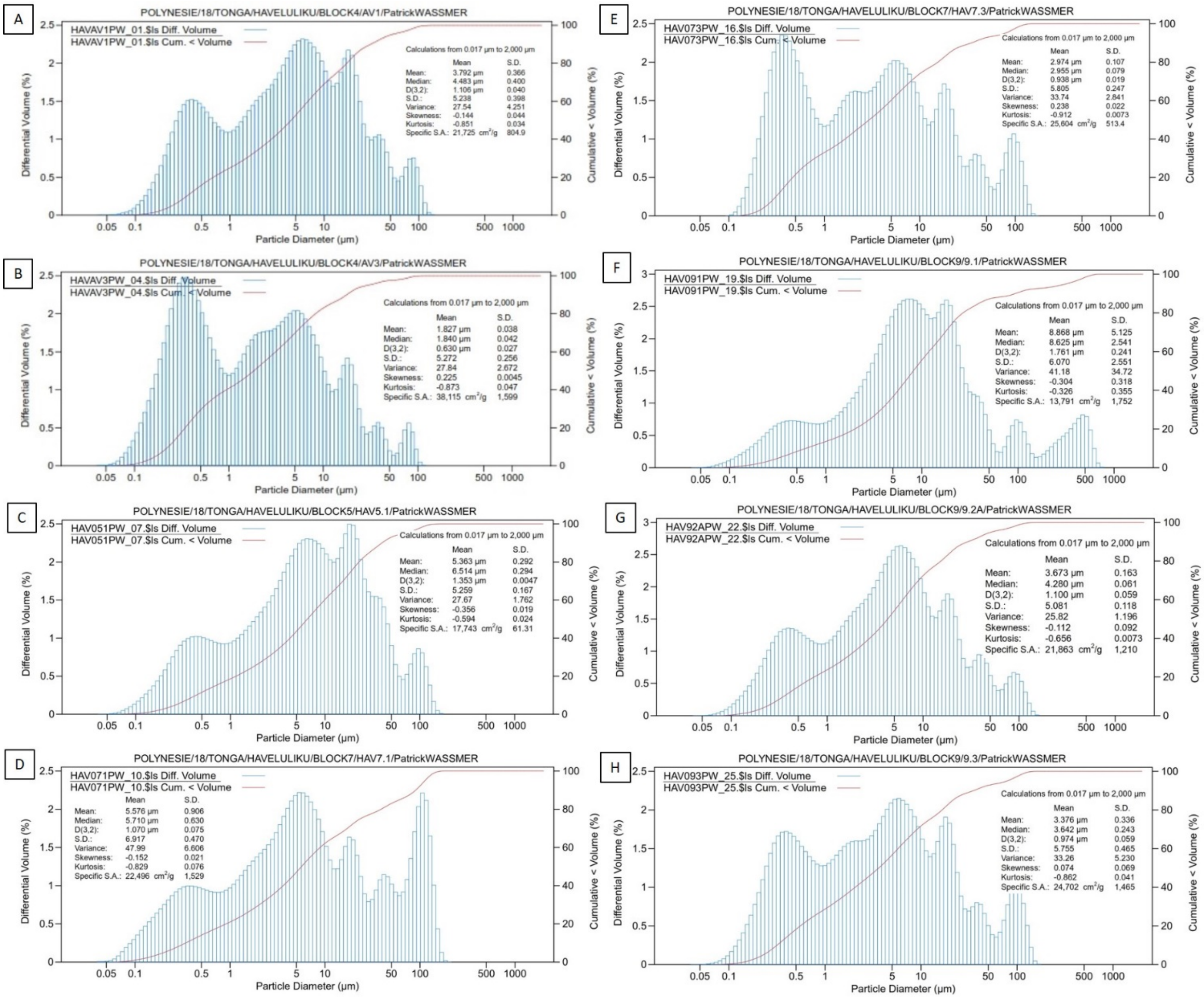

Fig. S2. Grain size of marine deposits under tsunami boulders at Haveluliku. The multimodal shape of the particle size curves indicates poor sorting due to an en-masse deposition by a highly turbulent flow, which was undoubtedly a large tsunami.

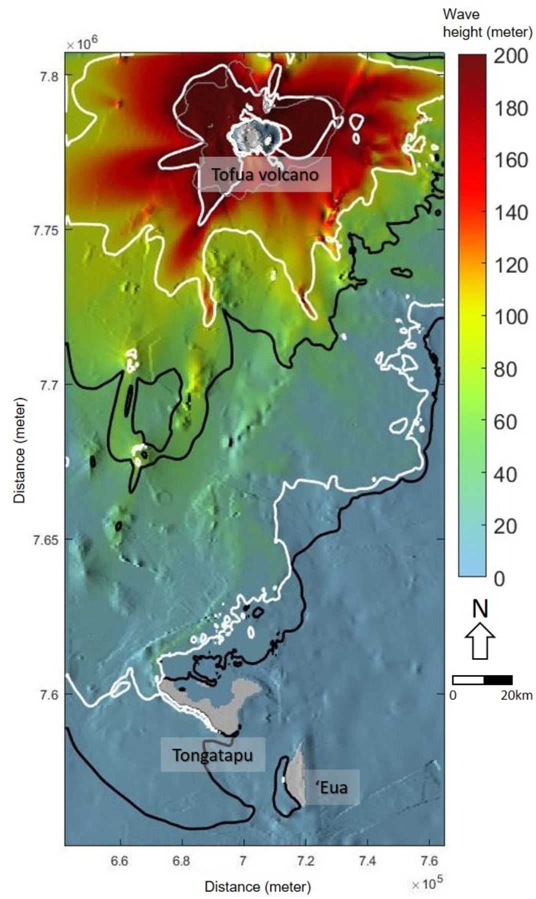

Fig. S3. Modelling of a tsunami triggered by voluminous debris avalanche entering the sea in the south flank of Tofua volcano. The shape of the Tofua caldera is a rim, 500 m in elevation and 8 km large. Based on the work of Caulfield et al. (2011), we reconstructed the pre-caldera shape of the volcano with an elevation of 2000 m, and simulated an immediate collapse of 74 km^3, which seems to be the worst case. We modeled this collapse with the two-fluid version of VolcFlow: the destabilisation is immediate but the mass accelerates according to the topography and the rheology, and does not enter immediately in the ocean. The collapse forms a debris avalanche that move underwater and reaches a distance of 30 km leaving a deposit 40 to 150 m thick. Close to Tofua, the main wave is more than 200 m high, but the amplitude rapidly decreases, following the inverse of the distance, because a volcano tsunami is generated very locally. Moreover, the shallow water of the Tonga Trench between Tofua and Tongatapu deflects the wave. At Tongatapu, the amplitude simulated is lower than 15 m and of only 5 m at the SE sector. Thus, it seems unlikely that the tsunami deposits observed at Haveluliku originated from Tofua.

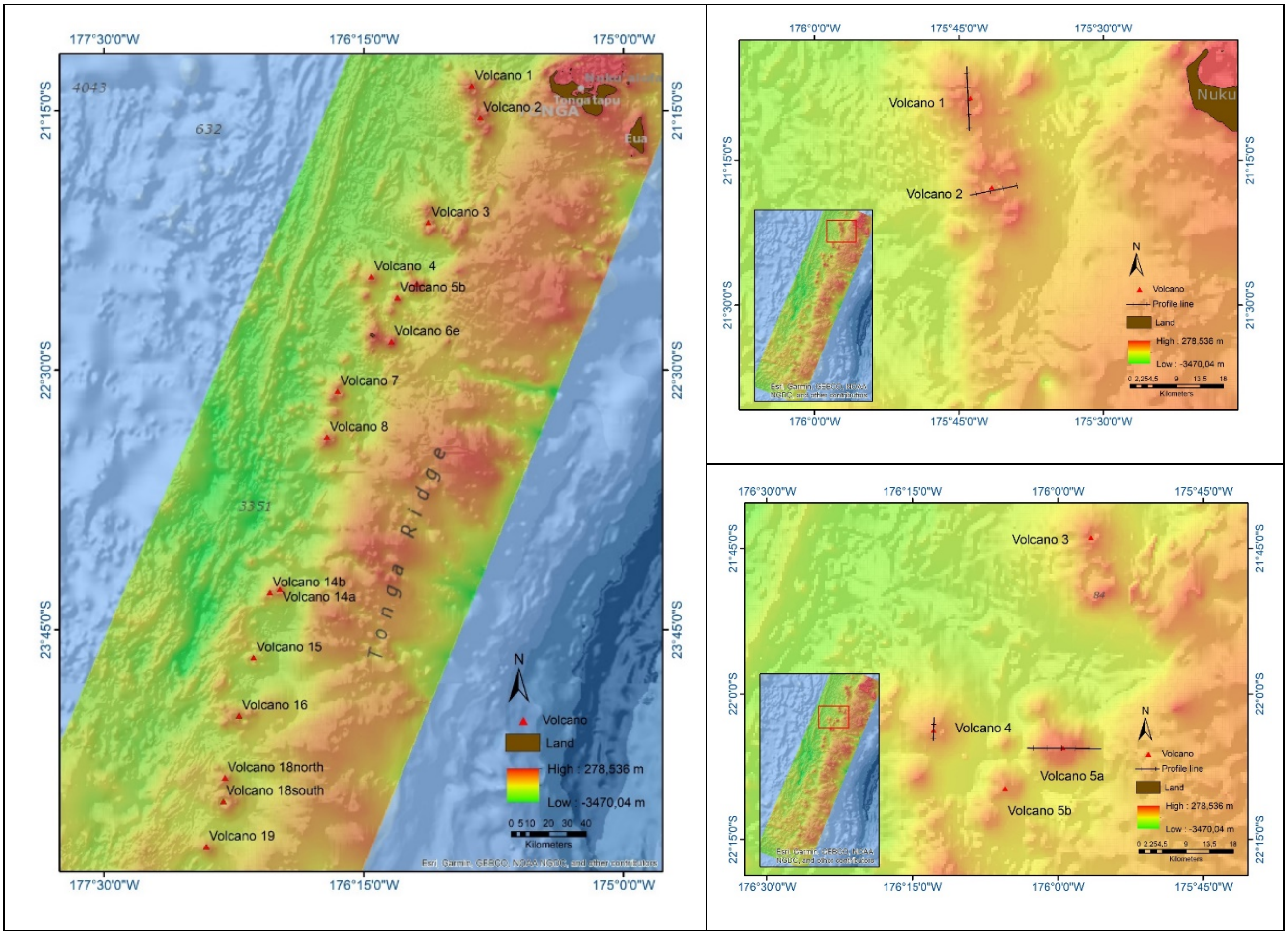

Fig. S4. Bathymetry of the South Tonga (Tofua) arc displayed in GMRT DEM, and location of the 15 calderas selected for this study, including cross-section lines. Volcano 1 and 2 are the closest from Tongatapu. Name and order of volcano based on Massoth et al., 2007.

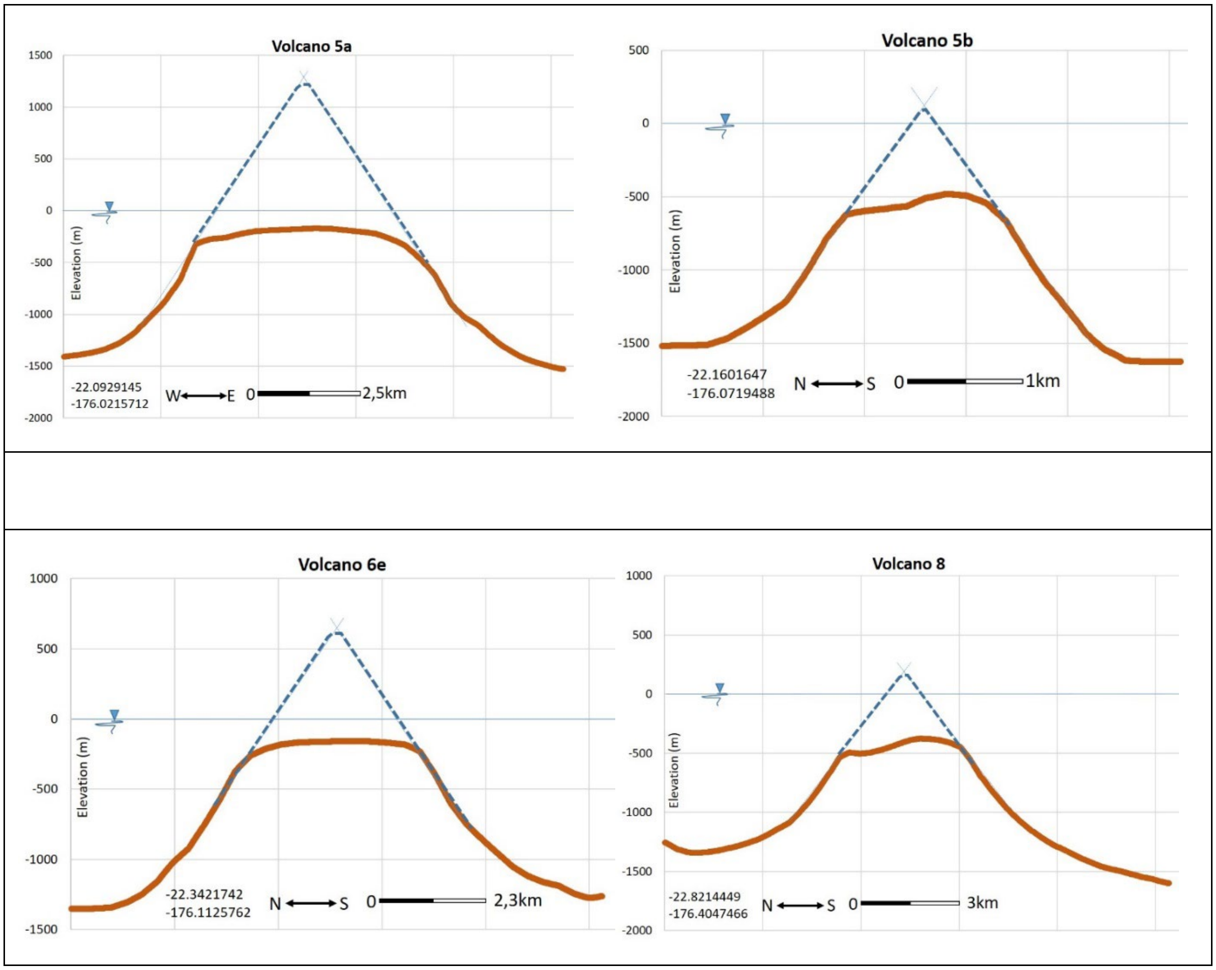

Figure S5. Underwater calderas resulting from the collapse of an ancient volcanic island. The 2D cross-section reconstructions show that 7 submarine calderas were formed as a result of the total collapse of former islands of varying elevation (4 examples are shown here). The highest was >1000 m (volcano 5a), and the lowest was < 250 m (volcano 5b). The other 5 volcanoes are in the same elevation range (500-650 m). With the highest elevation and widest caldera, volcano 5a is the best candidate to induce a tsunami, together with volcanoes 1 and 2

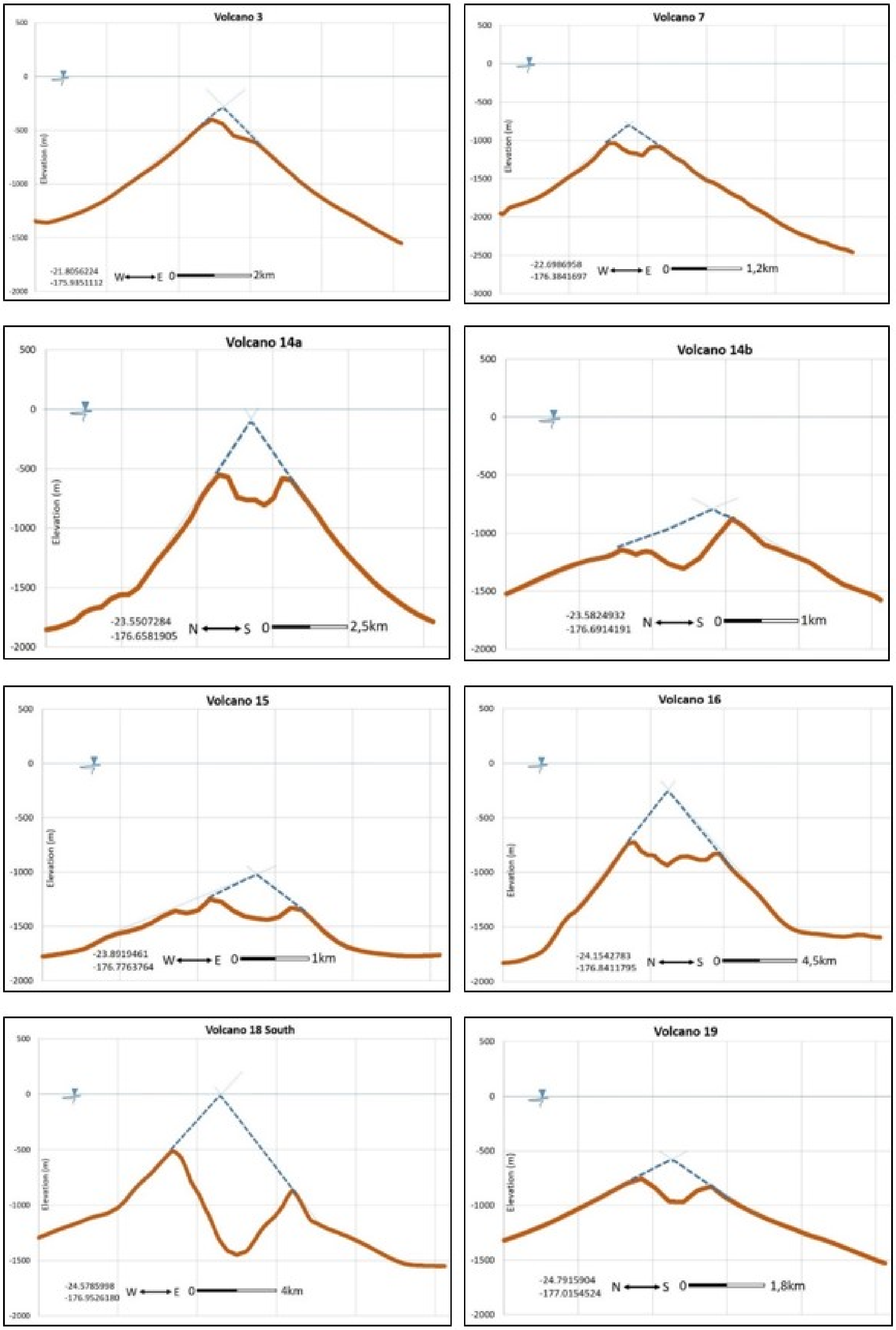

Figure S6. Underwater calderas formed by the collapse of an ancient submarine volcano. Eight submarine calderas of the Tonga range were formed by the collapse of a submarine volcano that was already submerged at the time of the caldera eruption. Reconstruction of the initial morphology of these submarine volcanoes shows that the diameter of the caldera is smaller than that of the formerly emerged volcanoes.

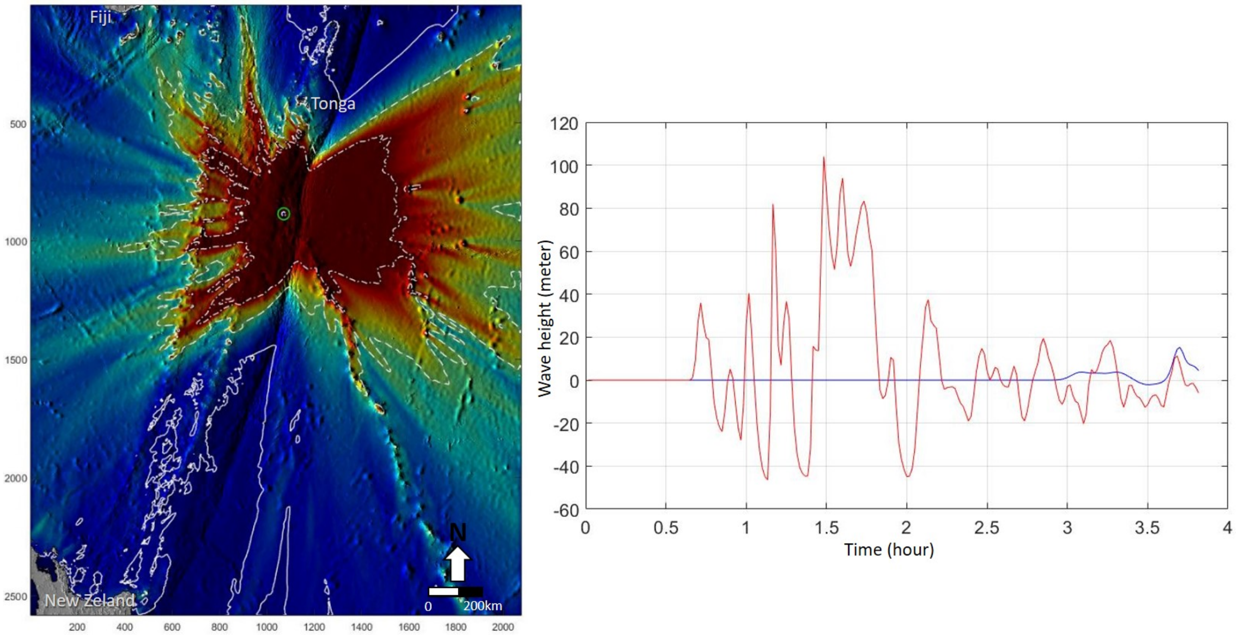

Fig. S7. Modelling of an impact-triggered tsunami from meteorite fall south of Tonga using Volcflow. Left: Tsunami modelling for a meteorite impact (green circle). The impact causes a displacement of the ocean following a spheroid with the height equalling the ocean depth at the impact (~3830 m) and a radius of 10 km. Right: Wave amplitudes recorded at Tongatapu (red) and at the North coast of New Zealand (blue). The huge initial wave strongly interacts with the bathymetry of the Tonga Trench and of the islands and a series of waves reaches the coasts. Fourty minutes after the impact, waves between 35 and 150 m in amplitude overflow the entire island of Tongatapu. New Zealand coasts are reached after 3 hours. The two waves observed is due to the bathymetry. The first wave travelled in the deep ocean to the East of the impact. It is fast, because the ocean is deep, but expands rapidly and decreases in amplitude. Its amplitude along the New Zealand coast is of about 5 m. The second wave moves along the west side of the Tonga Trench. It reaches the New Zealand coast 3h40 after the impact, with a wave amplitude exceeding 15 m.

Fig. S8. Monumental structures of two former capitals of the Tu'i Tonga Empire in Tongatapu. Left: Ha'amonga 'a Maui or trilithon at Heketā. Right: Mortuary structures at Lapaha. Radiocarbon dating of marine samples that have been collected beside the west upright of the trilithon provide ages of the monument construction between 1320 and 1460 CE (Clark and Reepmeyer, 2014), i.e. soon before the relocation of the Tu'i Tonga capital from Heketā to Lapaha.

2.2 Supplementary Tables

Table S1. Major and trace elements of pumice fragments within tsunami deposits

Sample's reference	SiO2	Al2O3	Fe2O3	MnO	MgO	CaO	Na2O	K2O	TiO2	P2O5	PF	Total
	%	%	%	%	%	%	%	%	%	%	%	%
AHONONOU1-C10	63,08	13,09	9,91	0,17	1,74	6,73	2,81	0,83	0,71	0,18	0,37	99,61
AHONONOU1-C13	63,48	13,22	9,71	0,17	1,73	6,42	2,73	0,78	0,70	0,18	1,06	100,18
AHONONOU1-C18-FC	66,00	13,77	6,63	0,15	1,64	5,83	3,09	0,63	0,57	0,19	1,35	99,86
AHONONOU1-C18-FF	67,37	13,27	6,27	0,15	1,18	5,11	3,38	0,64	0,52	0,16	1,62	99,67
AHONONOU1-C4-FF	58,18	14,35	11,82	0,19	2,86	8,15	2,44	0,72	0,76	0,16	0,10	99,72
AHONONOU1-C4-FGC	66,50	13,00	8,44	0,18	1,18	5,53	2,98	0,95	0,51	0,20	0,93	100,41
AHONONOU1-C4-Ocre	63,54	13,22	8,23	0,18	1,26	5,65	2,77	1,08	0,53	0,24	4,04	100,73
AHONONOU1-C6	66,66	12,50	8,91	0,16	1,08	5,65	2,83	0,63	0,47	0,15	1,70	100,75
AHONONOU1-C8-FC	67,12	12,59	6,60	0,15	1,14	5,53	2,89	0,79	0,54	0,18	1,78	99,30
AHONONOU1-C8-FF	61,52	12,81	9,83	0,17	1,77	7,05	2,72	0,80	0,70	0,18	1,31	98,86
AHONONOU2-C10-FC	65,70	14,32	4,83	0,14	1,05	4,70	3,86	0,85	0,55	0,15	2,40	98,56
AHONONOU2-C10-FF	66,43	12,43	7,49	0,17	1,17	5,23	2,92	0,79	0,45	0,18	2,20	99,45
AHONONOU2-C10-FTF	58,63	13,66	11,33	0,21	1,90	6,87	2,98	0,65	0,93	0,17	2,49	99,81
AHONONOU2-C2-FC	66,55	12,87	7,00	0,16	1,22	5,60	2,94	0,88	0,53	0,19	1,86	99,79
AHONONOU2-C2-FF	63,53	12,76	8,82	0,17	1,31	6,26	2,80	0,81	0,55	0,20	1,61	98,80
AHONONOU2-C2-FTF	62,05	13,05	10,05	0,17	1,92	6,85	2,75	0,81	0,71	0,18	0,56	99,10
AHONONOU2-C4-FC	67,52	13,32	5,88	0,14	1,12	5,08	3,23	0,83	0,55	0,16	1,39	99,20
AHONONOU2-C4-FF	60,74	13,58	9,94	0,19	1,94	6,72	2,61	0,88	0,63	0,22	2,04	99,49
AHONONOU2-C6-FC	65,36	13,30	8,12	0,18	1,20	5,33	3,06	1,14	0,54	0,24	0,80	99,26
AHONONOU2-C6-FF	61,47	13,31	10,32	0,17	1,80	6,58	2,70	0,80	0,74	0,18	1,33	99,39
AHONONOU2-C7	67,66	12,69	7,01	0,16	1,14	5,09	2,98	0,86	0,51	0,19	1,29	99,58
AHONONOU2-C9	64,20	13,19	7,59	0,18	1,33	5,22	3,37	1,12	0,62	0,21	1,79	98,80
ANAHULU1-AU-1-7-P	68,54	12,57	6,18	0,14	1,14	5,11	2,93	0,75	0,54	0,18	1,09	99,17
ANAHULU1-C16-FC	68,04	13,65	4,67	0,14	1,00	4,62	3,93	0,73	0,52	0,18	2,02	99,49
ANAHULU1-C16-FF	66,20	12,67	7,01	0,15	1,38	6,32	2,77	0,70	0,56	0,24	2,69	100,67
ANAHULU1-C18-Base-FC	68,93	12,70	6,30	0,14	1,18	5,30	2,94	0,74	0,54	0,17	1,37	100,31
ANAHULU1-C18-Base-FF	63,47	13,12	9,98	0,17	1,76	6,48	2,86	0,83	0,72	0,19	0,37	99,95
ANAHULU1-C18-Sup-FC	68,54	12,63	6,25	0,14	1,16	5,27	2,92	0,73	0,54	0,17	1,56	99,93
ANAHULU1-C18-Sup-FF	63,16	12,83	8,72	0,18	1,44	6,69	2,89	1,00	0,59	0,24	1,43	99,16
ANAHULU1-C2	67,11	12,26	7,43	0,16	1,06	5,32	2,88	0,67	0,44	0,20	1,15	98,67
ANAHULU3-EGS	63,34	12,84	8,41	0,16	1,69	6,08	2,70	0,74	0,59	0,18	1,96	98,68
TSUNAHULU1-D50-H8.6	65,27	12,65	4,07	0,14	1,05	6,06	4,01	0,64	0,46	0,18	5,62	100,15
HAVELULIKU-C1-BI5	65,30	12,82	9,22	0,17	1,12	5,93	2,71	0,61	0,49	0,16	1,44	99,97
KOLOVAI 1 (1/5)-FC	67,68	13,12	4,45	0,13	0,88	4,43	3,89	0,66	0,50	0,13	3,69	99,55
KOLOVAI 1 (1/5)-FF	68,04	12,33	6,08	0,10	1,36	5,34	3,20	0,76	0,37	0,12	1,78	99,49
KOLOVAI 1 (1/5)-FTF	64,92	12,24	8,80	0,17	1,16	6,23	2,76	0,67	0,50	0,16	1,54	99,14

Sample's reference	As	Ba	Be	Bi	Cd	Co	Cr	Cs	Cu	Ga	Ge	Hf	In	Mo	Nb	Ni	Pb	Rb	Sb	Sc	Sn	Sr
	µg/g	µg/g	µg/g	µg/g	µg/g	µg/g	µg/g	µg/g	µg/g	µg/g	µg/g	µg/g	µg/g	µg/g	µg/g	µg/g	µg/g	µg/g	µg/g	µg/g	µg/g	µg/g
AHONONOU1-C10	3,58	214	0,35	< L.D.	0,09	18,0	4,2	0,40	45,4	14,4	1,37	1,57	0,06	1,24	0,35	2,5	2,40	11,1	< L.D.	33,48	0,57	201
AHONONOU1-C13	3,73	213	0,32	0,05	0,11	17,4	4,8	0,37	47,4	14,6	1,40	1,55	0,07	1,21	0,35	2,9	2,45	11,0	< L.D.	33,24	0,61	206
AHONONOU1-C18-FC	4,14	180	0,31	< L.D.	0,11	10,6	17,4	0,46	28,6	13,6	1,36	1,73	0,06	1,40	0,38	4,0	2,52	8,94	0,10	26,94	0,60	161
AHONONOU1-C18-FF	5,04	182	0,42	< L.D.	0,11	8,46	4,6	0,59	20,7	13,8	1,40	1,89	0,06	2,05	0,45	2,1	2,96	8,89	0,14	24,40	0,66	181
AHONONOU1-C4-FF	3,79	184	0,32	< L.D.	0,10	27,0	5,1	0,42	174	15,8	1,43	1,38	0,06	1,30	0,30	7,2	3,20	8,94	< L.D.	38,68	0,51	261
AHONONOU1-C4-FGC	4,53	192	0,47	< L.D.	0,12	11,5	1,7	0,52	29,3	13,8	1,38	1,26	0,06	2,16	0,57	< L.D.	3,81	12,1	< L.D.	28,31	0,54	264
AHONONOU1-C4-Ocre	4,14	206	0,55	< L.D.	0,11	9,82	4,2	0,49	8,7	13,9	1,34	1,33	0,06	1,99	0,71	< L.D.	4,51	14,2	< L.D.	26,52	0,57	295
AHONONOU1-C6	5,82	150	0,33	< L.D.	0,10	13,1	1,4	0,50	49,1	13,4	1,37	1,13	0,06	2,48	0,32	< L.D.	3,02	7,76	< L.D.	29,41	0,43	221
AHONONOU1-C8-FC	3,97	209	0,33	< L.D.	0,11	8,99	5,4	0,37	42,0	13,1	1,40	1,46	0,06	1,33	0,38	2,2	2,77	11,1	0,09	25,91	0,53	202
AHONONOU1-C8-FF	3,71	210	0,35	0,06	0,12	18,3	6,3	0,39	44,7	14,0	1,29	1,56	0,06	1,23	0,34	3,4	2,41	11,0	< L.D.	32,94	0,59	231
AHONONOU2-C10-FC	3,56	276	0,56	0,09	0,11	4,98	3,2	0,93	6,7	14,5	1,54	2,69	0,07	1,63	0,73	< L.D.	3,71	15,9	0,12	17,61	0,81	182
AHONONOU2-C10-FF	5,28	171	0,43	< L.D.	0,11	9,55	1,8	0,49	18,0	12,7	1,50	1,27	0,07	2,41	0,44	< L.D.	3,47	9,81	0,13	26,70	0,49	247
AHONONOU2-C10-FTF	4,64	233	0,45	0,05	0,13	19,8	5,9	0,63	48,7	15,4	1,52	2,51	0,10	1,72	0,60	< L.D.	4,31	8,95	0,13	33,73	0,84	249
AHONONOU2-C2-FC	3,30	207	0,40	0,07	0,11	9,50	2,3	0,43	30,3	13,8	1,44	1,40	0,06	1,53	0,47	< L.D.	3,10	12,3	< L.D.	26,77	0,52	233
AHONONOU2-C2-FF	4,79	176	0,45	0,06	0,11	13,4	2,3	0,46	37,1	13,8	1,49	1,25	0,07	2,00	0,43	< L.D.	3,23	10,4	0,12	29,53	0,47	252
AHONONOU2-C2-FTF	3,25	204	0,36	0,05	0,11	19,0	10,0	0,41	49,0	14,7	1,54	1,47	0,08	1,22	0,33	2,9	2,35	11,1	0,06	34,58	0,51	197
AHONONOU2-C4-FC	3,00	238	0,40	< L.D.	0,12	7,49	2,1	0,58	29,4	13,7	1,48	1,83	0,07	1,21	0,46	< L.D.	2,82	13,5	0,17	23,41	0,63	166
AHONONOU2-C4-FF	3,86	189	0,45	0,05	0,12	16,3	4,1	0,43	30,9	14,7	1,48	1,32	0,08	1,53	0,51	< L.D.	3,42	11,9	0,08	32,92	0,64	272
AHONONOU2-C6-FC	3,96	213	0,60	0,07	0,12	9,89	1,3	0,54	15,7	14,5	1,54	1,36	0,08	2,11	0,72	< L.D.	4,22	15,0	0,10	26,71	0,56	288
AHONONOU2-C6-FF	3,33	209	0,36	< L.D.	0,11	18,9	2,6	0,42	48,6	14,6	1,53	1,54	0,08	1,23	0,34	< L.D.	2,54	11,3	0,06	34,19	0,56	205
AHONONOU2-C7	3,96	190	0,44	0,05	0,12	9,26	2,0	0,44	30,2	13,2	1,55	1,38	0,07	1,76	0,43	< L.D.	3,05	11,6	0,10	26,27	0,49	209
AHONONOU2-C9	3,31	244	0,69	0,06	0,13	9,39	2,1	0,64	17,6	14,8	1,57	2,35	0,08	1,91	0,95	< L.D.	4,28	16,9	0,09	25,11	0,79	266
ANAHULU1-AU-1-7-P	3,31	204	0,34	< L.D.	0,11	8,47	3,3	0,35	42,4	12,9	1,40	1,36	0,06	1,17	0,29	< L.D.	2,41	10,4	0,09	25,97	0,58	153
ANAHULU1-C16-FC	4,43	229	0,44	< L.D.	0,13	5,33	2,6	0,81	9,7	14,2	1,39	2,49	0,06	1,89	0,64	< L.D.	3,23	11,8	0,11	19,06	0,85	163
ANAHULU1-C16-FF	2,88	190	0,27	< L.D.	0,13	11,0	2,7	0,33	34,3	12,9	1,35	1,26	0,06	1,16	0,27	< L.D.	2,20	9,67	0,08	29,07	0,50	157
ANAHULU1-C18-Base-FC	3,56	203	0,26	< L.D.	0,12	8,83	3,5	0,36	41,4	13,0	1,38	1,38	0,06	1,28	0,30	2,8	2,39	10,5	0,09	26,70	0,52	152
ANAHULU1-C18-Base-FF	3,68	208	0,32	< L.D.	0,11	17,9	3,0	0,38	46,5	14,3	1,32	1,44	0,06	1,24	0,34	2,5	2,36	11,1	< L.D.	33,99	0,56	180
ANAHULU1-C18-Sup-FC	3,36	202	0,28	< L.D.	0,12	8,62	3,3	0,34	40,2	12,7	1,42	1,38	0,06	1,17	0,30	< L.D.	2,41	10,2	0,08	26,41	0,53	154
ANAHULU1-C18-Sup-FF	4,00	217	0,50	< L.D.	0,11	12,8	3,5	0,44	31,4	13,9	1,34	1,36	0,06	1,68	0,58	2,2	3,46	13,0	0,08	28,92	0,61	255
ANAHULU1-C2	5,92	147	0,40	< L.D.	0,11	9,12	1,2	0,49	25,5	12,3	1,42	1,18	0,07	2,48	0,32	< L.D.	3,10	8,19	0,15	26,82	0,46	221
ANAHULU3-EGS	4,75	184	0,30	0,05	0,15	13,8	5,2	0,41	41,6	13,0	1,31	1,38	0,06	1,69	0,34	3,9	3,43	9,88	0,11	30,30	0,59	195
TSUNAHULU1-D50-H8.6	4,50	188	0,47	< L.D.	0,14	3,99	1,7	0,69	13,0	13,8	1,40	2,57	0,07	2,00	0,64	< L.D.	3,35	8,88	0,13	17,27	0,80	208
HAVELULIKU-C1-BI5	6,14	154	0,31	0,05	0,11	14,0	4,7	0,45	55,0	13,3	1,36	1,15	0,06	2,35	0,32	2,1	6,91	7,51	0,38	30,17	0,48	230
KOLOVAI 1 (1/5)-FC	5,04	189	0,44	0,05	0,12	4,43	1,7	0,77	9,2	13,8	1,49	2,49	0,08	2,10	0,56	< L.D.	3,49	9,66	0,13	19,34	0,75	170
KOLOVAI 1 (1/5)-FF	3,70	162	0,49	< L.D.	0,07	11,0	7,0	0,43	50,9	11,1	1,29	1,33	0,04	2,00	2,00	2,6	3,12	11,6	0,16	21,17	0,42	194
KOLOVAI 1 (1/5)-FTF	5,85	144	0,36	< L.D.	0,12	12,3	1,5	0,45	40,9	12,5	1,41	1,10	0,07	2,25	0,34	< L.D.	3,21	8,11	0,12	29,21	0,42	254

Sample's reference	Ta	Th	U	V	W	Y	Zn	Zr	La	Ce	Pr	Nd	Sm	Eu	Gd	Tb	Dy	Ho	Er	Tm	Yb	Lu
	µg/g	µg/g	µg/g	µg/g	µg/g	µg/g	µg/g	µg/g	µg/g	µg/g	µg/g	µg/g	µg/g	µg/g	µg/g	µg/g	µg/g	µg/g	µg/g	µg/g	µg/g	µg/g
AHONONOU1-C10	0,03	0,31	0,23	170	< L.D.	24,8	105	43,5	3,16	8,22	1,38	7,39	2,52	0,854	3,15	0,580	4,03	0,944	2,73	0,429	2,82	0,452
AHONONOU1-C13	0,03	0,32	0,22	160	< L.D.	24,7	105	43,1	3,10	8,26	1,36	7,23	2,55	0,841	3,16	0,581	4,08	0,957	2,70	0,433	2,88	0,448
AHONONOU1-C18-FC	0,03	0,37	0,20	83,4	< L.D.	28,3	89,2	45,7	3,05	8,25	1,38	7,73	2,73	0,911	3,52	0,657	4,57	1,07	3,06	0,483	3,15	0,509
AHONONOU1-C18-FF	0,04	0,40	0,23	54,8	< L.D.	29,9	94,0	53,0	3,32	8,99	1,55	8,23	2,99	0,956	3,74	0,688	4,85	1,14	3,27	0,519	3,42	0,534
AHONONOU1-C4-FF	0,03	0,27	0,24	285	< L.D.	22,0	111	36,7	2,57	6,90	1,18	6,43	2,27	0,793	2,82	0,534	3,66	0,843	2,37	0,373	2,46	0,388
AHONONOU1-C4-FGC	0,05	0,37	0,33	52,4	< L.D.	20,6	116	35,3	3,45	8,40	1,37	7,06	2,30	0,771	2,75	0,493	3,45	0,786	2,23	0,358	2,36	0,374
AHONONOU1-C4-Ocre	0,06	0,45	0,38	50,1	< L.D.	20,2	115	37,3	3,99	9,72	1,54	7,85	2,48	0,828	2,82	0,501	3,34	0,766	2,19	0,336	2,32	0,374
AHONONOU1-C6	0,03	0,22	0,24	53,6	< L.D.	20,3	108	30,7	2,28	6,00	1,03	5,60	1,97	0,669	2,47	0,474	3,34	0,770	2,24	0,359	2,38	0,385
AHONONOU1-C8-FC	0,03	0,34	0,24	52,8	< L.D.	25,1	95,0	36,6	3,11	7,82	1,27	6,87	2,40	0,832	3,10	0,585	4,10	0,958	2,80	0,435	2,91	0,463
AHONONOU1-C8-FF	0,03	0,31	0,24	174	0,81	24,5	104	42,6	3,09	8,10	1,36	7,26	2,49	0,846	3,11	0,570	3,97	0,930	2,70	0,416	2,77	0,456
AHONONOU2-C10-FC	0,07	1,17	0,39	28,7	< L.D.	32,0	75,6	77,6	5,77	15,0	2,36	12,0	3,71	1,12	4,26	0,765	5,27	1,21	3,43	0,539	3,66	0,570
AHONONOU2-C10-FF	0,04	0,29	0,29	38,1	< L.D.	21,0	109	33,4	2,86	7,26	1,23	6,47	2,19	0,736	2,68	0,495	3,38	0,783	2,27	0,361	2,46	0,398
AHONONOU2-C10-FTF	0,06	0,56	0,28	126	< L.D.	32,1	111	67,6	3,93	11,1	1,88	10,1	3,45	1,12	4,22	0,785	5,36	1,20	3,42	0,538	3,53	0,550
AHONONOU2-C2-FC	0,04	0,38	0,29	47,4	< L.D.	23,8	102	35,4	3,35	8,26	1,36	7,18	2,46	0,828	3,06	0,570	3,92	0,898	2,60	0,411	2,70	0,425
AHONONOU2-C2-FF	0,04	0,30	0,28	84,0	< L.D.	20,8	106	33,6	2,89	7,36	1,24	6,48	2,17	0,732	2,66	0,489	3,42	0,787	2,28	0,366	2,45	0,388
AHONONOU2-C2-FTF	0,03	0,31	0,23	186	< L.D.	24,1	99,8	38,6	3,00	7,89	1,34	7,12	2,44	0,823	3,04	0,570	3,98	0,918	2,66	0,415	2,81	0,439
AHONONOU2-C4-FC	0,04	0,68	0,29	46,7	< L.D.	26,6	80,8	48,4	4,01	10,1	1,62	8,32	2,75	0,884	3,33	0,624	4,34	0,996	2,89	0,461	3,07	0,479
AHONONOU2-C4-FF	0,04	0,38	0,31	111	< L.D.	20,4	111	34,7	3,30	8,31	1,35	6,99	2,29	0,786	2,69	0,499	3,40	0,777	2,24	0,351	2,37	0,375
AHONONOU2-C6-FC	0,06	0,45	0,38	43,0	< L.D.	20,7	120	37,2	4,05	9,67	1,57	8,02	2,51	0,845	2,85	0,508	3,47	0,783	2,25	0,354	2,38	0,379
AHONONOU2-C6-FF	0,03	0,34	0,23	174	< L.D.	24,5	105	40,4	3,08	8,23	1,38	7,32	2,52	0,847	3,10	0,582	4,02	0,936	2,68	0,426	2,81	0,450
AHONONOU2-C7	0,04	0,34	0,27	43,1	< L.D.	23,0	97,7	33,6	3,10	7,72	1,31	6,93	2,37	0,791	2,97	0,541	3,78	0,876	2,52	0,404	2,68	0,424
AHONONOU2-C9	0,08	0,92	0,48	48,8	< L.D.	27,7	110	67,3	6,19	15,5	2,44	12,1	3,60	1,10	3,99	0,693	4,69	1,06	3,04	0,480	3,17	0,499
ANAHULU1-AU-1-7-P	0,03	0,31	0,21	50,1	< L.D.	25,3	88,6	35,6	2,80	7,18	1,19	6,60	2,44	0,783	3,02	0,600	4,22	0,980	2,84	0,450	2,99	0,470
ANAHULU1-C16-FC	0,06	0,71	0,29	23,5	< L.D.	35,6	84,8	73,8	4,66	12,4	2,06	11,0	3,68	1,14	4,40	0,812	5,72	1,33	3,74	0,577	3,90	0,638
ANAHULU1-C16-FF	0,02	0,29	0,20	79,4	< L.D.	23,9	92,8	33,0	2,63	6,62	1,11	6,10	2,22	0,755	2,82	0,537	3,84	0,917	2,63	0,400	2,74	0,450
ANAHULU1-C18-Base-FC	0,03	0,31	0,20	51,8	< L.D.	25,5	87,2	35,5	2,83	7,20	1,18	6,42	2,30	0,794	3,08	0,592	4,23	0,978	2,82	0,446	2,97	0,467
ANAHULU1-C18-Base-FF	0,03	0,30	0,22	171	< L.D.	23,8	103	41,8	2,99	7,86	1,31	7,05	2,37	0,799	2,89	0,557	3,95	0,901	2,54	0,413	2,74	0,430
ANAHULU1-C18-Sup-FC	0,02	0,32	0,20	51,1	< L.D.	25,4	88,4	35,8	2,79	7,13	1,20	6,38	2,31	0,779	2,98	0,592	4,17	0,970	2,78	0,437	2,96	0,465
ANAHULU1-C18-Sup-FF	0,10	0,37	0,31	95,3	< L.D.	21,4	116	39,5	3,66	9,04	1,47	7,63	2,46	0,827	2,85	0,528	3,66	0,833	2,41	0,379	2,51	0,396
ANAHULU1-C2	0,03	0,23	0,26	36,3	< L.D.	20,4	107	31,3	2,32	6,07	1,05	5,61	1,97	0,673	2,49	0,467	3,26	0,752	2,21	0,357	2,40	0,383
ANAHULU3-EGS	0,03	0,28	0,24	106	< L.D.	22,8	114	37,5	2,77	7,24	1,19	6,44	2,28	0,743	2,77	0,527	3,70	0,854	2,47	0,386	2,60	0,421
TSUNAHULU1-D50-H8.6	0,06	0,46	0,28	16,3	< L.D.	35,8	88,4	74,2	3,87	11,2	1,95	10,5	3,69	1,16	4,50	0,838	5,95	1,37	3,94	0,619	4,03	0,654
HAVELULIKU-C1-BI5	0,03	0,22	0,23	66,2	< L.D.	20,1	114	32,5	2,31	6,06	1,02	5,59	1,99	0,678	2,44	0,457	3,27	0,779	2,22	0,353	2,39	0,380
KOLOVAI 1 (1/5)-FC	0,05	0,59	0,27	20,1	< L.D.	36,5	75,9	65,1	3,86	11,0	1,89	10,2	3,59	1,12	4,53	0,859	5,94	1,38	3,96	0,624	4,17	0,651
KOLOVAI 1 (1/5)-FF	0,12	0,72	0,43	89,6	< L.D.	16,4	64,9	38,1	3,87	8,08	1,17	5,49	1,67	0,515	2,04	0,378	2,60	0,606	1,76	0,281	1,94	0,305
KOLOVAI 1 (1/5)-FTF	0,03	0,22	0,25	55,3	< L.D.	19,3	107	29,1	2,27	5,87	1,03	5,44	1,85	0,641	2,35	0,444	3,10	0,735	2,10	0,333	2,27	0,363

Table S2. Major elements of pumice glass within tsunami deposits

Matrix glass analysis													
FileName : A17P.qtiDat													
Column Conditions : Cond 1 : 15keV 6nA													
Date : 10-Oct-2019													
Beam Size : 10 µm													
Compositions normalised to 100%, free of volatiles													
Sample A17P-1 (layer 18 Anahulu - Fig. 5)													
DataSet/Point	SiO2	TiO2	Al2O3	FeO	MnO	MgO	CaO	Na2O	K2O	P2O5	Cl	Total	Tot Alkalis
1 / 1.	73,36	0,53	12,31	4,93	0,15	0,65	4,34	2,74	0,87	0,13	0,2597	98,79	3,61
2 / 1.	72,89	0,53	11,97	5,42	0,14	1,02	4,40	2,64	0,86	0,14	0,2223	98,01	3,50
4 / 1.	73,54	0,51	12,34	4,90	0,10	0,61	4,24	2,72	0,89	0,14	0,2185	98,38	3,61
6 / 1.	73,67	0,55	12,32	4,63	0,15	0,64	4,18	2,81	0,89	0,15	0,2307	95,72	3,70
7 / 1.	74,17	0,52	12,28	4,63	0,15	0,60	4,14	2,52	0,85	0,14	0,2081	98,85	3,37
9 / 1.	73,44	0,50	12,26	4,89	0,18	0,68	4,23	2,81	0,87	0,14	0,2378	98,29	3,68
17 / 1.	73,87	0,58	12,05	4,91	0,20	0,64	4,14	2,56	0,88	0,17	0,247	96,81	3,44
18 / 1.	74,03	0,48	12,20	4,60	0,16	0,68	4,25	2,54	0,89	0,17	0,2355	97,42	3,43
20 / 1.	73,67	0,55	12,26	4,80	0,12	0,65	4,25	2,62	0,90	0,18	0,2261	97,94	3,52
21 / 1.	73,01	0,54	12,09	5,19	0,10	0,81	4,38	2,89	0,84	0,16	0,2641	98,57	3,72
22 / 1.	73,02	0,53	12,14	5,14	0,12	0,88	4,47	2,72	0,85	0,15	0,2665	98,18	3,56
23 / 1.	73,03	0,48	11,89	5,26	0,15	1,10	4,61	2,52	0,81	0,16	0,2368	98,79	3,33
24 / 1.	73,06	0,48	12,34	4,91	0,24	0,78	4,39	2,77	0,87	0,17	0,2247	98,55	3,64
25 / 1.	73,82	0,51	12,20	4,72	0,16	0,66	4,10	2,78	0,88	0,17	0,2136	98,61	3,66
26 / 1.	73,09	0,54	12,06	5,16	0,15	0,76	4,33	2,92	0,82	0,16	0,3037	98,06	3,74
27 / 1.	73,79	0,56	11,61	5,19	0,12	0,79	4,16	2,79	0,83	0,14	0,3048	98,09	3,63
28 / 1.	70,74	0,46	13,39	4,89	0,14	1,04	5,54	2,90	0,75	0,14	0,1917	99,57	3,65
29 / 1.	73,42	0,53	12,56	4,63	0,10	0,66	4,27	2,80	0,88	0,15	0,2152	97,73	3,68
31 / 1.	72,93	0,54	12,20	5,23	0,12	0,83	4,40	2,70	0,87	0,17	0,2256	96,99	3,56
32 / 1.	73,10	0,55	12,08	5,10	0,14	0,80	4,45	2,74	0,83	0,21	0,2197	98,18	3,57
33 / 1.	71,52	0,54	11,42	6,28	0,24	1,58	4,75	2,68	0,82	0,17	0,2253	97,13	3,51
34 / 1.	73,53	0,52	11,82	5,04	0,19	0,75	4,36	2,77	0,87	0,14	0,246	96,29	3,64
35 / 1.	72,05	0,57	11,98	5,59	0,11	1,17	4,94	2,67	0,80	0,14	0,2055	99,07	3,46
36 / 1.	73,53	0,50	12,39	4,60	0,10	0,77	4,31	2,79	0,81	0,20	0,2147	98,34	3,59
37 / 1.	73,47	0,52	12,26	5,02	0,13	0,71	4,11	2,67	0,92	0,19	0,2015	97,53	3,59
38 / 1.	73,89	0,52	12,26	4,70	0,05	0,61	4,14	2,74	0,89	0,18	0,2283	95,48	3,63
Average (n= 26)	**73,22**	**0,52**	**12,18**	**5,01**	**0,14**	**0,80**	**4,38**	**2,72**	**0,85**	**0,16**	**0,23**		**3,58**
STD	**0,77**	**0,03**	**0,35**	**0,37**	**0,04**	**0,22**	**0,31**	**0,11**	**0,04**	**0,02**	**0,03**		**0,11**
Sample KOL1-A (Kolovai)													
DataSet/Point	SiO2	TiO2	Al2O3	FeO	MnO	MgO	CaO	Na2O	K2O	P2O5	Cl	Total	
1 / 1.	74,71	0,45	13,41	3,19	0,08	0,49	3,35	3,44	0,76	0,11	0,2263	98,06	4,20
2 / 1.	74,28	0,47	13,11	3,59	0,22	0,64	3,55	3,29	0,74	0,11	0,1857	98,58	4,03
4 / 1.	75,71	0,44	12,69	3,45	0,10	0,46	3,04	3,22	0,82	0,07	0,1919	93,58	4,04
5 / 1.	75,59	0,45	12,70	3,41	0,15	0,59	3,12	3,11	0,79	0,10	0,1845	98,39	3,89
6 / 1.	74,82	0,41	13,74	2,71	0,10	0,34	3,34	3,69	0,78	0,08	0,2092	95,65	4,47
7 / 1.	73,98	0,47	13,02	3,88	0,06	0,93	3,63	3,17	0,77	0,09	0,1933	98,09	3,94
8 / 1.	74,73	0,48	13,26	3,48	0,07	0,58	3,47	3,11	0,74	0,09	0,1993	99,50	3,85
9 / 1.	74,15	0,45	13,17	3,67	0,17	0,69	3,43	3,41	0,76	0,09	0,1914	98,36	4,17
10 / 1.	74,56	0,47	13,28	3,45	0,14	0,62	3,37	3,27	0,75	0,11	0,2001	98,07	4,02
11 / 1.	75,10	0,42	13,17	3,20	0,09	0,51	3,29	3,39	0,74	0,11	0,1891	98,17	4,13
12 / 1.	74,92	0,44	12,95	3,58	0,10	0,72	3,23	3,17	0,80	0,08	0,2164	97,11	3,97
13 / 1.	72,10	0,47	12,43	5,10	0,15	1,63	4,08	3,17	0,75	0,12	0,1723	98,74	3,92
14 / 1.	74,32	0,52	13,11	3,69	0,18	0,54	3,53	3,21	0,79	0,11	0,1855	98,99	4,00
16 / 1.	75,77	0,44	12,93	3,15	0,06	0,50	3,21	3,17	0,74	0,02	0,1888	99,35	3,92
18 / 1.	74,38	0,46	13,25	3,54	0,13	0,64	3,49	3,21	0,77	0,11	0,1823	98,41	3,98
19 / 1.	74,22	0,41	13,80	3,16	0,07	0,48	3,42	3,63	0,76	0,05	0,1873	99,44	4,39
20 / 1.	74,72	0,49	13,24	3,33	0,16	0,55	3,41	3,25	0,78	0,07	0,1948	96,60	4,03
22 / 1.	74,91	0,43	13,49	2,94	0,12	0,47	3,45	3,34	0,76	0,10	0,1726	100,20	4,10
23 / 1.	74,97	0,42	13,23	3,42	0,08	0,55	3,28	3,17	0,76	0,13	0,3054	92,10	3,93
24 / 1.	74,49	0,49	13,15	3,22	0,14	0,67	3,52	3,40	0,81	0,10	0,1724	97,69	4,21
25 / 1.	74,92	0,44	13,12	3,12	0,19	0,47	3,30	3,58	0,77	0,09	0,1916	99,09	4,35
Average (n= 21)	**74,64**	**0,45**	**13,15**	**3,44**	**0,12**	**0,62**	**3,41**	**3,30**	**0,77**	**0,09**	**0,20**		**4,07**
STD	**0,76**	**0,03**	**0,32**	**0,47**	**0,05**	**0,26**	**0,21**	**0,17**	**0,02**	**0,02**	**0,03**		**0,17**

Sample KOL1-B (Kolovai)													
DataSet/Point	SiO2	TiO2	Al2O3	FeO	MnO	MgO	CaO	Na2O	K2O	P2O5	Cl	Total	
1 / 1.	74,71	0,35	11,82	4,48	0,11	0,79	3,71	2,99	0,93	0,12	0,1771	98,53	3,92
2 / 1.	69,15	0,46	11,55	8,72	0,15	1,44	5,26	2,47	0,66	0,15	0,2036	98,55	3,13
3 / 1.	70,47	0,48	11,92	7,79	0,09	0,84	5,03	2,54	0,70	0,14	0,2287	97,68	3,24
4 / 1.	75,57	0,35	11,61	4,52	0,11	0,66	3,28	2,81	0,98	0,11	0,1745	99,03	3,79
5 / 1.	75,34	0,34	11,66	4,39	0,18	0,66	3,43	2,85	0,99	0,14	0,1782	98,40	3,84
6 / 1.	70,66	0,51	12,02	7,53	0,18	0,81	4,91	2,47	0,75	0,17	0,2363	97,85	3,22
7 / 1.	69,99	0,44	12,39	7,33	0,24	0,83	5,14	2,77	0,68	0,19	0,2261	98,68	3,44
8 / 1.	70,67	0,44	12,11	7,25	0,28	0,81	4,94	2,60	0,71	0,18	0,2234	97,66	3,31
9 / 1.	75,06	0,38	11,76	4,41	0,00	0,73	3,70	2,85	0,95	0,16	0,152	99,21	3,81
10 / 1.	74,90	0,31	11,88	4,54	0,08	0,74	3,68	2,82	0,92	0,12	0,1868	98,46	3,74
11 / 1.	75,40	0,37	11,56	4,30	0,09	0,65	3,48	3,06	0,94	0,15	0,1706	98,08	4,00
12 / 1.	75,36	0,36	11,78	4,35	0,13	0,66	3,54	2,78	0,96	0,08	0,1677	98,45	3,74
13 / 1.	75,38	0,35	11,57	4,50	0,14	0,67	3,49	2,89	0,90	0,12	0,2067	96,30	3,78
14 / 1.	75,72	0,37	11,43	4,34	0,03	0,69	3,49	2,86	0,96	0,13	0,1843	97,85	3,82
15 / 1.	70,32	0,49	12,16	7,50	0,24	0,84	5,03	2,55	0,71	0,17	0,2338	98,94	3,26
16 / 1.	75,94	0,38	11,49	4,22	0,03	0,60	3,43	2,85	0,97	0,09	0,1824	98,97	3,81
17 / 1.	75,54	0,38	11,71	4,25	0,13	0,71	3,38	2,82	0,96	0,14	0,1537	99,07	3,78
18 / 1.	70,50	0,42	12,03	7,60	0,17	0,83	5,00	2,51	0,75	0,20	0,2375	98,66	3,26
19 / 1.	75,14	0,36	11,71	4,58	0,14	0,71	3,54	2,77	0,94	0,12	0,167	98,98	3,71
20 / 1.	70,57	0,46	12,18	7,30	0,16	0,80	4,96	2,65	0,73	0,19	0,2292	98,42	3,37
22 / 1.	75,06	0,37	11,86	4,52	0,01	0,70	3,51	2,96	0,89	0,12	0,1561	98,66	3,86
23 / 1.	75,16	0,37	11,66	4,58	0,04	0,70	3,47	2,88	0,98	0,17	0,1654	97,81	3,86
24 / 1.	70,22	0,49	11,99	7,68	0,16	0,88	5,11	2,56	0,73	0,17	0,2132	97,73	3,29
25 / 1.	70,72	0,49	12,00	7,35	0,18	0,80	4,93	2,64	0,73	0,17	0,2382	98,70	3,37
Average (n= 24)	**73,23**	**0,40**	**11,83**	**5,75**	**0,13**	**0,77**	**4,14**	**2,75**	**0,85**	**0,15**	**0,20**		**3,60**
STD	**2,54**	**0,06**	**0,25**	**1,62**	**0,07**	**0,16**	**0,77**	**0,17**	**0,12**	**0,03**	**0,03**		**0,28**

Sample KOL1-C (Kolovai)													
DataSet/Point	SiO2	TiO2	Al2O3	FeO	MnO	MgO	CaO	Na2O	K2O	P2O5	Cl	Total	
1 / 1.	69,90	0,51	12,17	7,83	0,22	0,83	5,23	2,46	0,70	0,17	0,2305	98,37	3,16
2 / 1.	69,89	0,51	12,16	7,75	0,15	0,92	5,10	2,64	0,72	0,16	0,2308	98,37	3,36
3 / 1.	70,66	0,49	11,95	7,60	0,16	0,68	4,81	2,67	0,79	0,19	0,2337	98,89	3,46
5 / 1.	70,41	0,48	12,04	7,51	0,17	0,89	5,02	2,59	0,72	0,18	0,2237	97,60	3,31
8 / 1.	70,59	0,48	11,93	7,44	0,13	0,90	4,87	2,79	0,69	0,18	0,2133	93,78	3,48
9 / 1.	70,26	0,49	12,04	7,61	0,16	0,86	4,97	2,68	0,72	0,21	0,234	98,55	3,41
11 / 1.	70,14	0,50	12,08	7,64	0,17	0,90	5,00	2,73	0,71	0,14	0,2162	98,46	3,44
12 / 1.	70,18	0,48	11,88	7,66	0,22	0,88	5,10	2,71	0,70	0,19	0,2605	98,49	3,42
13 / 1.	69,84	0,49	12,07	7,71	0,12	0,91	5,16	2,77	0,73	0,20	0,222	98,59	3,50
14 / 1.	68,65	0,44	13,88	6,54	0,14	0,69	6,10	2,76	0,63	0,17	0,1812	98,52	3,39
15 / 1.	70,49	0,49	12,02	7,42	0,12	0,85	5,01	2,68	0,74	0,19	0,228	98,62	3,41
16 / 1.	70,38	0,49	12,07	7,45	0,10	0,84	5,13	2,66	0,71	0,16	0,2097	98,99	3,38
17 / 1.	70,48	0,50	11,99	7,51	0,13	0,91	5,05	2,55	0,71	0,17	0,238	97,93	3,26
18 / 1.	70,17	0,48	12,25	7,39	0,22	0,91	5,00	2,65	0,73	0,18	0,2157	98,33	3,38
20 / 1.	70,05	0,48	11,85	7,97	0,12	0,87	5,13	2,57	0,73	0,22	0,2457	97,99	3,30
21 / 1.	70,03	0,48	12,11	7,63	0,09	0,88	5,15	2,72	0,73	0,17	0,2354	99,01	3,46
23 / 1.	70,07	0,48	11,88	8,01	0,20	0,85	5,20	2,48	0,71	0,12	0,2367	99,79	3,19
24 / 1.	69,61	0,49	11,99	8,01	0,19	0,91	5,23	2,68	0,70	0,20	0,2651	97,59	3,38
25 / 1.	70,29	0,49	12,15	7,36	0,18	0,81	5,10	2,80	0,71	0,12	0,2367	98,82	3,50
26 / 1.	70,19	0,48	12,09	7,60	0,28	0,82	5,03	2,63	0,70	0,18	0,2359	98,24	3,33
27 / 1.	69,96	0,45	12,23	7,79	0,12	0,90	5,00	2,63	0,71	0,20	0,2261	98,68	3,34
Average (n= 21)	**70,11**	**0,48**	**12,14**	**7,59**	**0,16**	**0,86**	**5,11**	**2,66**	**0,71**	**0,18**	**0,23**		**3,37**
STD	**0,43**	**0,02**	**0,42**	**0,31**	**0,05**	**0,07**	**0,25**	**0,09**	**0,03**	**0,03**	**0,02**		**0,09**

Table S3. Characteristic of tsunami boulders in Tongatapu

	Boulder	Latitude (La)	Longitude (Lo)	Altitude (A)	Length (Le)	Width (Wi)	Height (H)	Volume (V)	Density (D)*	Weigth (We)	Flow velocity	Flow depth (free boulder scenario)	
				(m asl)	*(m)*	*(m)*	*(m)*	*π.Le.Wi.H/6 m^3*	*kg/m3*	*tons*	*m/s (free boulders)*	*m (Fr=0.75)*	*m (Fr=1.0)*
Fahefa	1	21°08'05,10	175°20'40,50	10	15	11	9	777	2000	1554	11,4	23,6	13,2
West coast	2	21°08'02,77	175°20'35,03	14,5	4,5	2,5	3,6	21	2000	42	4,5	3,7	2,1
	3	21°08'35,05	175°20'26,98	15,5	12,5	3	3,6	71	2000	141	5,2	4,9	2,8
	4	21°08'45,54	175°20'24,02	16,5	4,6	4	2	19	2000	39	7,8	11,0	6,2
	5	21°09'00,52	175°20'24,02	17,5	6	4,5	2,5	35	2000	71	8,1	11,9	6,7
	6	21°08'40,63	175°20'20,10	21,5	6	4,5	2,5	35	2000	71	8,1	11,9	6,7
	7	21°09'11,58	175°20'16,08	13,5	13	7,1	4,8	232	2000	464	9,7	17,1	9,6
Haveluliku	1	21°12'16,52	175°06'16,52	32	3,5	2	1,2	4	2000	9	5,3	5,1	2,9
SE coast	2	21°12'16,51	175°06'16,44	32	5	4	2	21	2000	42	7,8	11,0	6,2
	3	21°12'16,51	175°06'16,44	32	4	2	1,7	7	2000	14	4,8	4,2	2,3
	4	21°12'16,50	175°06'15,92	31	3,8	2,6	1,7	9	2000	18	5,9	6,3	3,5
	5	21°12'16,50	175°06'15,92	31	1,5	1	1	1	2000	2	3,2	1,9	1,0
	6	21°12'16,50	175°06'15,92	31	2	1	1,2	1	2000	3	3	1,6	0,9
	7	21°12'16,49	175°06'15,92	31	4	3	1	6	2000	13	7,1	9,1	5,1
	8	21°12'16,48	175°06'15,66	31	8	3	3,2	40	2000	80	5,4	5,3	3,0
	9	21°12'16,45	175°06'14,87	30	6,5	2,5	1,3	11	2000	22	6,1	6,7	3,8

* based on Spiske et al., 2008

SI References

Caulfield, J. T., Cronin, S. J., Turner, S. P., and Cooper, L. B. (2011). Mafic Plinian volcanism and ignimbrite emplacement at Tofua volcano, Tonga. *Bull. Volcanol.* 73, 1259–1277. doi:10.1007/s00445-011-0477-9.

Clark, G., and Reepmeyer, C. (2014). Stone architecture, monumentality and the rise of the early Tongan chiefdom. *Antiquity* 88, 1244–1260. doi:10.1017/S0003598X00115431.

Karátson D., Yepes J., Rodriguez-Peces M.J., Favalli M., Fornaciai A., 2016 Reconstructing eroded paleovolcanoes on Gran Canaria, Canary Islands, using advanced geomorphometry. *Geomorphology* 253, 123-134. Doi:10.1016/j.geomorph.2015.10.004

Lahitte P., Samper A., Quidelleur X., 2012. DEM-based reconstruction of southern Basse-Terre volcanoes (Guadeloupe archipelago, FWI): Contribution to the Lesser Antilles Arc construction rates and magma production. *Geomorphology* 136, 1, 148-164. doi:10.1016/j.geomorph.2011.04.008.

Massoth, G., Baker, E., Worthington, T., Lupton, J., De Ronde, C., Arculus, R., et al. (2007). Multiple hydrothermal sources along the south Tonga arc and Valu Fa Ridge. *Geochemistry, Geophys. Geosystems* 8. doi:10.1029/2007GC001675.

Petchey, F., and Clark, G. (2011). Tongatapu hardwater: Investigation into the 14C marine reservoir offset in lagoon, reef and open ocean environments of a limestone island. *Quat. Geochronol.* 6, 539–549. doi:10.1016/j.quageo.2011.08.001.

Stuiver, M., Reimer, P.J., and Reimer, R.W. (2021). CALIB 8.2 [WWW program] at http://calib.org, accessed 2021-7-25